Localization of the Center of Intramuscular Nerve Dense Regions in Deltoid Muscle: An Applied Anatomical Study

Localización del Centro de las Regiones Intramusculares Densamente Inervadas en el Músculo Deltoides: Un Estudio Anatómico Aplicado

Songling Ji¹; Huaixiang Luo¹; Sifeng Wen² & Shengbo Yang¹

JI, S.; LUO, H.; WEN, S. & YANG, S. Localization of the center of intramuscular nerve dense regions in deltoid muscle: An applied anatomical study. *Int. J. Morphol.*, 43(5):1747-1753, 2025.

SUMMARY: Accurately locating the central intramuscular nerve dense region (CINDR) within the deltoid muscle is essential for safe and effective intramuscular drug injections. Improper targeting increases the risk of nerve injury, whereas accurate localization provides valuable guidance for routine drug injections and specific botulinum toxin therapy. This study examined 24 adult cadavers to determine the location of the CINDR within the deltoid muscle. A longitudinal reference line (L-line) was drawn between the acromion and lateral epicondyle of the humerus, and a semicircular transverse reference line (H-line) was drawn from the lowest point of the jugular notch, passing through the acromion to the medial end of the scapular spine. Sihler's staining was used to visualize the intramuscular nerve-dense regions, and barium sulfate was applied to mark the CINDR. Spiral computed tomography (CT) scans and the Syngo system were used to record the projection point of the CINDR on the body surface, designated as point P. The intersection of the vertical line through point P with the H-line and the horizontal line with the L-line were designated as PH and PL, respectively. The percentage positions of PH and PL along the H-line and L-line, as well as the depth of the CINDR were measured and analyzed. The anterior, middle, and posterior parts of the deltoid muscle contained a distinct intramuscular nerve-dense area. The PH points of the CINDR were located at 45.52 %, 54.76 %, and 76.19 % along the H-line, whereas the PL points were located at 18.99 %, 23.65 %, and 22.16 % along the L-line. The CINDR depths were 1.08 cm, 1.99 cm, and 1.44 cm, respectively. All percentages represent mean values. The identified CINDR locations should be avoided during routine intramuscular drug injections and should serve as effective targets for botulinum toxin-based shoulder slimming procedures and the treatment of muscle spasms.

KEY WORDS: Deltoid Muscle; Injections; Intramuscular nerves; Botulinum Toxins; Tomography; Spiral computed tomography.

INTRODUCTION

In addition to its roles in shoulder abduction, flexion/extension, and rotation, the deltoid muscle also contributes to joint stabilization (Lewis *et al.*, 2016). It is a common site for intramuscular injections. However, all medications possess inherent neurotoxicity, and injecting them into regions with dense intramuscular nerve distribution poses a risk of iatrogenic neural injury from the procedure (Kakati *et al.*, 2013). Significant damage to nerves innervating the deltoid muscle can lead to impaired shoulder abduction and even square shoulder deformity (Van Gelein Vitringa *et al.*, 2011). Deltoid muscle hypertrophy may occur due to genetic factors, overtraining, or pathological conditions. In women seeking aesthetic improvements, such hypertrophy can result

in the loss of a soft, feminine physique (Koh et al., 2023; Yi et al., 2023). Botulinum toxin (BoNT) injection has emerged as a minimally invasive approach for reshaping the deltoid muscle contour, offering advantages such as procedural simplicity, rapid recovery, and minimal adverse effects (Shin et al., 2021; Yi et al., 2024). Many central nervous system diseases, such as stroke, traumatic brain injury, spinal cord injury, and amyotrophic lateral sclerosis, can lead to secondary muscle spasticity (Picelli et al., 2017). When such spasticity affects the deltoid muscle, it may result in shoulder joint dislocation, restricted movement, or shoulder pain (Van Ouwenaller et al., 1986; Pinho et al., 2023). Intramuscular injection of BoNT for treating muscle spasticity is an

FUNDED. National Natural Science Foundation of China, Grant/Award Number: 32260217.

Received: 2025-08-01 Accepted: 2025-08-16

¹Department of Anatomy Zunyi Medical University, Zunyi City, Guizhou Province, China.

²Department of Basic Medicine Zunyi Medical University, Zunyi City, Guizhou Province, China.

increasingly popular approach that works by inhibiting acetylcholine release at motor endplates and blocking neural transmission to the muscle (Shin *et al.*, 2021; Yi *et al.*, 2023). The action site of BoNTs resides at the motor endplates; however, staining and localization of these structures are limited by the availability of fresh specimens. Given the topological consistency between intramuscular nerve dense regions (INDRs) and motor endplate bands, INDRs can serve as a surrogate targeting site (Amirali *et al.*, 2007; He *et al.*, 2022, 2025).

Since the aforementioned clinical issues are associated with intramuscular nerve distribution, this study aimed to employ a modified Sihler's staining method to elucidate the overall distribution pattern of intramuscular nerves in the deltoid muscle. Additionally, the CINDRs were precisely localized using spiral CT scanning. This approach was designed to provide safer and more effective targeting sites for deltoid muscle injections, BoNT-based shoulder slimming procedures, and management of deltoid muscle spasticity. We hypothesized that the deltoid muscle contained consistent INDRs that could be reliably identified through anatomical staining and imaging, thereby supporting safer and more targeted injection strategies.

MATERIAL AND METHOD

Specimens and ethics: This study was performed on 24 adult cadavers (12 men and 12 women), aged 30-75 years at the time of death, with no history of neuromuscular disease or shoulder deformity. Among them, 12 cadavers (six males and six females) were fixed in formalin, while the other 12 (six males and six females) were freshly collected and cryopreserved. The collection and use of specimens were approved by the ethics committee of our school (Ethical approval: #2022-1-003).

Gross anatomy: Each cadaver was placed in the lateral decubitus position. Semicircular incisions were made at the root of the neck and mid-humerus, followed by a longitudinal incision extending from the acromion process along the lateral margin of the arm to the mid-humerus. The skin and subcutaneous tissues were carefully reflected both anteriorly and posteriorly along the muscle surface to expose the deltoid muscle and quadrilateral space. This allowed observation of the axillary nerve branches and their points of intramuscular entry. Intact deltoid muscles from 12 cadavers (six males and six females) were harvested for Sihler's intramuscular nerve staining.

Reference line design: A longitudinal reference line (L-line) was defined as the connection between the acromion (point a) and the lateral epicondyle of the humerus (point b) to

facilitate the description of the positional relationship between the CINDR and superficial bony landmarks. A semicircular horizontal reference line (H-line) was established from the lowest point of the jugular notch (point c), passing through the acromion to the medial end of the spine of the scapula (point d).

Sihler's staining method showed INDRs: The excised deltoid muscles were processed following a modified Sihler's staining protocol (Hu et al., 2024): Depigmentation: Incubated in a solution of 3 % potassium hydroxide and 0.2 % hydrogen peroxide for 3-4 weeks; Decalcification: Immersed in Sihler's Solution I for 4 weeks; Staining: Treated with Sihler's Solution II for 4 weeks; Decolorization: Transferred to Sihler's Solution I for 3-24 h: Neutralization: Rinsed in 0.05 % lithium carbonate solution for 1-2 h with agitation; Clearing: Gradually dehydrated in a glycerol gradient (40-100 %) for 1 week each. The intramuscular nerve branch distribution was observed using an X-ray film viewer, photographed, and used to generate schematic diagrams. The percentage positions of the INDR along the length and width of the muscle were measured using Vernier calipers.

Localization of CINDR by spiral CT: The skin and subcutaneous fat of frozen cadavers were incised en bloc to expose the deltoid muscles. Based on the results of Sihler's staining (with three INDRs identified in the deltoid muscle), the CINDRs were located within the deltoid muscle, and barium sulfate mixed with a glue was injected for marking. Needles were then inserted at bony landmarks on the body surface, and a barium sulfate-soaked silk thread was sutured tightly against the skin between the needles to represent the reference lines. Spiral CT scanning and three-dimensional reconstruction were performed, followed by measurement using the Syngo system. The projection points of the CINDRs on the body surface were named points $P(P_1, P_2, P_3)$ and P₂). Perpendicular lines were drawn from each P point to the L-line with their intersections named $P_L(P_{1L}, P_{2L}, P_{3L})$; similarly, perpendicular lines were drawn from each P point to the H-line with their intersections named $P_L(P_{1H}, P_{2H},$ and P_{3H}). The lengths of the L-line, a-P_L, H-line, and c-P_H lines, as well as the absolute depths of the CINDRs, were measured. The percentiles were calculated as a-P₁/L and c-P_H/H values.

Statistical analysis: SPSS17.0 (IBM Corporation, Armonk, NY, USA) software was used for data analysis. The experimental data were expressed as $(x\pm s)$ % to eliminate the influence of individual differences. A paired t-test was used to compare the data between the right and left muscles. The comparison between men and women was performed using a two-sample t-test, test level was $\alpha = 0.05$.

RESULTS

Gross anatomical observation: The deltoid muscle can be divided into the anterior, middle (lateral), and posterior parts. After passing through the quadrilateral foramen, the axillary nerve typically divides into 3-5 branches, accompanied by the posterior humeral circumflex vessels, which enter the deep surface of the muscle at the mid-upper portion of its length and midpoint of its width. Three patterns of axillary nerve branching were observed in the deltoid muscle: The 4-branch type was the most common (91.67 %, 22/24). The anterior and posterior parts of the muscle are supplied by 1 branch, whereas the middle (lateral) part is supplied by two branches. The 3-branch type accounted for 4.16 % (1/24) of cases, with the anterior, middle, and posterior parts receiving one branch each. The 5-branch type accounted for 4.16 %(1/24), where the anterior and posterior parts were supplied by two branches, and the middle (lateral) part was supplied by one branch (Fig. 1). Additionally, the anterolateral part of the deltoid muscle received dual innervation from the lateral pectoral nerve in 79.17 % (19/24) of cases.



Fig. 1. Gross Anatomical Study of Common Nerve Supply Patterns to the Deltoid Muscle. 1=anterior bundles of the deltoid muscle; 2=middle bundles of the deltoid muscle; 3=posterior bundles of the deltoid muscle

Modified Sihler's staining method for displaying intramuscular nerve dense region: After entering the deltoid muscle, the axillary nerve demonstrates distinct branching patterns in different regions. The branches supplying the anterior muscle fibers typically ran horizontally, giving off arborizing branches upward and

downwards. The branches supplying the middle muscle fibers ran downwards, fanning out and giving off the arborizing branches. The branches supplying the posterior muscle fibers first ran horizontally backward and then gave off arborizing branches downwards along their course. These arborizing branches formed three INDRs within the muscle: the INDR1 was located at $(26.73 \pm 1.93) \% - (45.96 \pm 2.33)$ % of the muscle length and (17.58 \pm 1.67) % - (35.68 \pm 2.19) % of the muscle width, covering an area of (4.5 \pm 0.02) cm². The INDR2 (middle region) spanned (39.15 \pm (2.77) % - (46.41 ± 3.02) % of the muscle length and (39.59) ± 4.02) % - (60.56 ± 4.54) % of the muscle width, with an area of (2.61 ± 0.03) cm². The INDR3 (posterior region) occupied (14.03 ± 1.6) % - (40.17 ± 2.45) % of the muscle length and (63.83 ± 5.01) % - (82.03 ± 6.18) % of the muscle width, measuring (4.32 ± 0.03) cm² (Fig. 2). Notably, a horizontal band-like neural distribution spanned (14.03 ± 1.6) % - (46.41 ± 3.02) % of the muscle length and $(17.58 \pm$ 1.67) % - (82.03 ± 6.18) % of the muscle width.

The branches of the lateral pectoral nerve entered the deltoid muscle from its deep surface and, after penetrating the muscle, traversed the anterior margin from the midpoint of the muscular substance, branching along their path. These rami did not form a distinct, dense nerve plexus within the muscles.

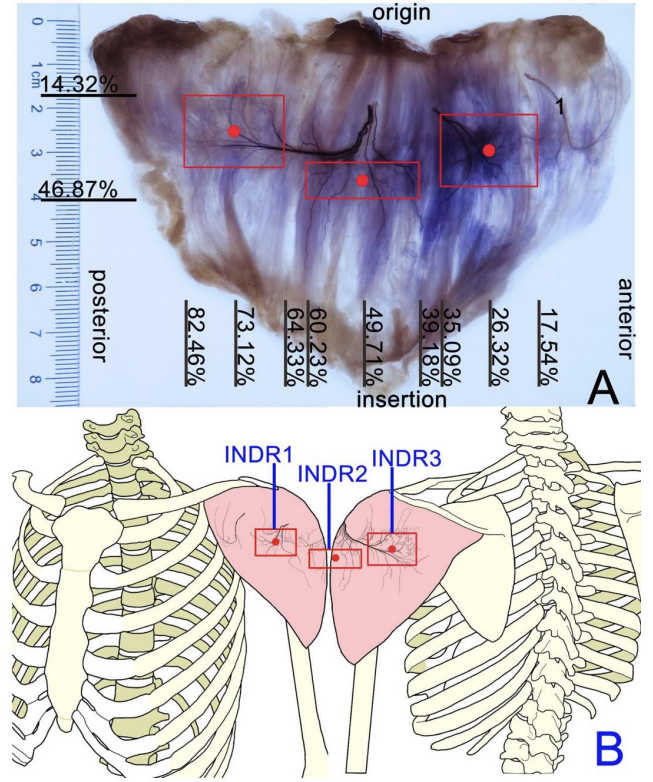


Fig. 2. Intramuscular nerve distribution pattern in the deep aspect of left deltoideus and location of CINDR. A: Sihler's Staining. Red box and dot represented INDR and CINDR respectively. 1=Lateral pectoral nerve. Bar, cm. B: Schematic drawing of Figure A.

Spiral CT localization of the CINDR: The CINDRs marked with barium sulfate, along with reference lines and bony landmarks, appeared in white on both the surface and tomographic images reconstructed from the spiral CT. The projection of the CINDRs onto the skin indicates the puncture site (point P) for needle insertion. The position at which the CINDR projects onto the L reference line can be measured in the coronal plane, whereas its position and depth on the H reference line can be determined in the axial plane. In this study, a CT localization image of the anterior part of the deltoid muscle is shown as an example (Fig. 3A-3D). The percentage positions and depths of the CINDR projections for lines H and L are detailed in Table I. Statistical analysis showed no significant differences (P > 0.05) between the left and right sides or between the male and female subjects (Tables II and III).

Table I. The percentage position of the PH and PL of CINDR of deltoideus on Lines H and L respectively and depth of CINDR $(x\pm s)$

CINDR	P _L on line	P _L on line	P-CINDR
	L (%)	H (%)	(cm)
CINDR ₁	18.59±1.25	45.04±3.05	1.03±0.17
CINDR ₂	23.50 ± 2.16	55.09±1.59	2.01±0.14
CINDR ₃	21.78 ± 1.36	76.00 ± 1.81	1.51±0.15

DISCUSSION

The deltoid muscle is innervated by the axillary nerve (Stokey *et al.*, 2024). The predominant branching pattern of the axillary nerve before entering the deltoid muscle, characterized by a four-branch configuration (Stecco *et al.*, 2010), aligns with our findings. Larionov etal. (2020), reported that >80 % of the anterior fibers of the deltoid muscle received additional innervation from the lateral pectoral nerve. In our study involving 24 deltoid muscles, dual innervation from the lateral pectoral nerve was observed in 19 specimens, demonstrating a strong concordance with the findings of Larionov *et al.* (2020).

Iatrogenic nerve injuries caused by intramuscular injections are not related to mechanical trauma from the needle; they are primarily attributable to neurotoxicity-induced degeneration and necrosis of nerves and muscles (Gentili *et al.*, 1980; Pandian *et al.*, 2006; Cohen & Gray, 2010; Desai *et al.*, 2019). As a common site for intramuscular injections, the deltoid muscle has been the focus of multiple safety guidelines aimed at preventing nerve damage. For instance, injecting medications 5-7 cm below the acromion, within 31-43 % of the muscle length, has been shown to avoid major nerve trunk injury (Kim *et al.*, 2022; Stokey *et al.*, 2024). Considering muscle thickness, some protocols recommend administering injections slightly below the

Table II. Comparison of the P_{u} and P_{t} positions on the H and L lines and the depth of CINDRs in deltoideus muscle between males and females ($x \pm x$, n=24 sides.

	$P_{ m L}$ on Ii	$P_{\rm L}$ on line L (%)			$P_{\rm L}$ on I	P_{L} on line H (%)			Q	Depth of CINDR (cm)	(cm)	
CINDRs	male	female		a	male	Female	,	a	male	female	,	۵
	(n=12)	(n=12)	•	ı,	(n=12)	(n=12)	7	,	(n=12)	(n=12)	7	,
CINDR1	19.19 ± 1.30	17.99 ± 0.87	2.642	0.165	45.54 ± 3.33	44.55 ± 2.80	62.0	0.518	1.03 ± 0.19	1.05 ± 0.14	-0.324	0.369
CINDR2	24.12 ± 1.74	22.89 ± 2.16	1.530	0.657	55.34 ± 0.99	54.85 ± 1.93	0.79	0.119	2.02 ± 0.15	2.00 ± 0.12	0.410	0.336
CINDR3	22.05 ± 1.48	21.51 ± 0.88	1.077	0.197	76.29 ± 1.34	75.72 ± 2.12	0.793	0.616	1.52 ± 0.16	1.51 ± 0.09	0.17	0.094

des.	
=24 si	
±s, n=	
\mathbf{x}	
t side	
l righ	
ft and	
the le	
een 1	
betw	
uscle	
eus m	
ltoid	
in de	
CINDRs	
f CIN	
epth c	
the do	
s and	
line	
and L	
the H and	
s on t	
sition	
PL po	
and I	
le PH	
ı of th	
arisor	
Comp	
le III. C	
Table	
-	

	Ь	0.89	0.89	0.67
)Rs	t	0.131	0.129	-0.427
Depth of CINDRs	Right side (n=12)	1.03 ± 0.16	2.01 ± 0.14	1.52 ± 0.16
P _H on line H (H'/H%)	Left side $(n=12)$	1.03 ± 0.18	2.01 ± 0.13	1.50 ± 0.15
	Ь	0.237	0.478	0.105
	t	-1.214 0.237	-0.722	-1.688
	Right side (n=12)	45.15 ± 3.24	55.17 ± 1.65	76.17 ± 1.86
	Left side (n=12)	44.93±2.91	55.02 ± 1.55	75.84 ± 1.78
	Ь	0.264	0.690	0.369
$P_{\rm L}$ on line L (%)	t	-1.145	-0.404	-0.917
	Right side $(n=12)$	18.65 ± 1.25	23.57 ± 2.00	21.90 ± 1.47
	Left side (n=12)	18.53 ± 1.28	23.43 ± 2.35	21.67 ± 1.26
	CINDRs	CINDR	$CINDR_2$	CINDR

99

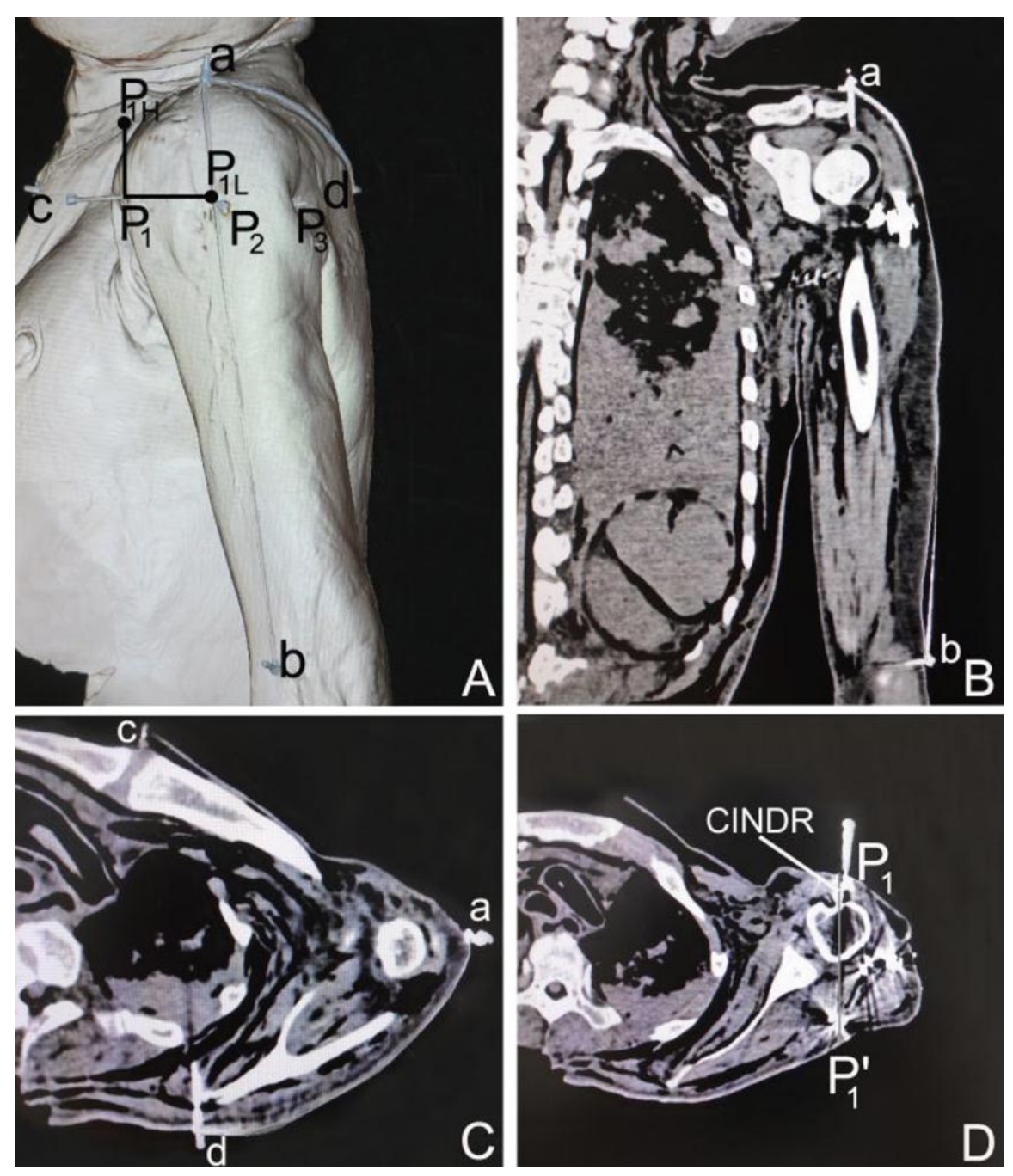


Fig. 3. Spiral CT localization image of the CINDR of the left deltoid muscle. A: Spiral CT three-dimensional reconstruction image showing the projection positions of the CINDR on the body surface along with the designed reference lines. B: Measurement of the length of line L on the coronal section. C: Measurement of the length of line H on the cross section. D: Measurement of the depth of the CINDR on the cross section.

midpoint of the muscle (7 cm below the acromion). Conversely, for adults, administering medications 10 cm below the acromion (60 % of the muscle length) helps circumvent vascular and neural structures (Charmode *et al.*, 2022). Three INDRs were identified based on the intramuscular nerve distribution results of this study: the

anterior part at 18.82-41.12 % of muscle length, the middle part at 37.65-48.24 %, and the posterior part at 25.88-47.06 %. These findings suggest that these INDRs should be avoided during intramuscular injections into the deltoid muscle to prevent nerve damage and associated functional impairments.

However, when administering intramuscular BoNT injections for muscle spasticity or shoulder contour improvement, precise targeting of the neuromuscular junction is essential to block acetylcholine release, thereby alleviating muscle spasms and inducing muscular atrophy. Therefore, precise localization of INDR is critical, as deviation of the BoNT injection site by more than 5 mm from the motor endplate results in a 50 % reduction in therapeutic efficacy (Parratte et al., 2002). Numerous studies have reported the use of BoNT injections targeting the deltoid muscle. A previous study suggested an approach in which multi-point injections were administered along the course of the anterior branch of the axillary nerve within the deltoid muscle, 5-6 cm below the acromion (Gentili et al., 1980); another proposed multi-point injections at the mid-upper 1/3 intersection of the muscle length in the central deltoid, with additional injections at the midlower 1/3 intersection for the anterior and posterior regions (Yi et al., 2023); and another recommended eight-point injections within a 2×5 cm² area under the acromion (Koh et al., 2023). However, such multipoint injections increase patient burden owing to higher costs, procedural pain, antibody formation, and muscle fibrosis risk (Wang et al., 2022, 2024). Additionally, electrostimulation-guided targeting via surface stimulation of the adult deltoid muscle, which identified sites eliciting maximal muscular contraction as injection points, revealed five horizontally distributed motor points that formed a band (Behringer et al., 2014). However, that study employed different reference lines (the anterior-posterior axillary fold line (X-axis) and the acromion-anterior axillary fold line (Yaxis)), precluding a direct comparison with our findings. Our research demonstrated a horizontal band-like neural distribution within 14.03-82.03 % of the muscle length, encompassing three intramuscular neural dense regions. After marking the central points with barium sulfate and performing spiral CT scanning, we precisely localized these regions along two defined reference lines. These anatomical landmarks can reduce the need for multiple injections, thereby minimizing dosage and patient discomfort. Regarding the BoNT injection dose for the deltoid muscle, both Shin et al. (2021) and Pinho et al. (2023) recommended a dose of 50U during cosmetic or spasticity treatments of the deltoid muscle. Koh et al. (2023) compared two groups of patients with deltoid muscle cosmetic concerns who received 16U and 32U injections, respectively. The results revealed that both groups achieved arm circumference reduction, although there was no statistically significant difference in the degree of reduction. However, the 16U low-dose group exhibited fewer side effects, suggesting that 16U was sufficient to achieve therapeutic effects. Efficacy did not increase proportionally beyond this dose. Based on the recommended infiltration of 1.5-3 cm² per BTX-A unit and 4.5 cm² per 2.5-5 units (Borodic *et al.*, 1994), combined with the recommended INDR area of INDR, INDR₂, and INDR3 identified in this study, it is estimated that

only 3U, 1U, and 3U of BoNT, respectively, are needed for these three regions to achieve therapeutic effects. This approach significantly reduces the total BoNT injection dose.

By marking the CINDR with barium sulfate and performing spiral CT scans with three-dimensional reconstruction, we established reliable mediolateral and superior-inferior relationships between internal nerve targets and surface bony landmarks. These reference-based coordinates can help guide more accurate and safer injections into the deltoid muscle. However, the study has certain limitations, including a relatively small sample size, a lack of racial diversity, exclusive use of adult cadavers without pediatric representation, and the absence of clinical validation. These factors may affect the generalizability of our findings and highlight the need for further validation across broader populations.

CONCLUSION

This study accurately mapped the intramuscular nerve distribution of the deltoid muscle using Sihler's staining and CT-based localization, enabling precise identification of CINDR. These findings have important clinical implications for improving the safety and efficacy of BoNT injections and intramuscular drug delivery. Future research should focus on validating these anatomical landmarks through ultrasound-guided clinical applications.

ACKNOWLEDGMENTS. We are grateful for the support from the National Natural Science Foundation of China, Grant/Award Number: 32260217. The authors sincerely thank those who donated their bodies to science so that anatomical research could be performed. Results from such research can potentially increase human-kind overall knowledge that can then improve patient care. Therefore, these donors and their families deserve our highest gratitude.

CJI, S.; LUO, H.; WEN, S. & YANG, S. Localización del centro de las regiones intramusculares densamente inervadas en el músculo deltoides: Un estudio anatómico aplicado. *Int. J. Morphol.*, 43(5):1747-1753, 2025.

RESUMEN: La localización precisa de la región central intramuscular densamente inervada (RCDNI) en el músculo deltoides es fundamental para la seguridad y eficacia de las inyecciones intramusculares de fármacos. Una punción incorrecta aumenta el riesgo de lesión nerviosa, mientras que una localización precisa proporciona una guía valiosa para las inyecciones rutinarias de fármacos y la terapia específica con toxina botulínica. Este estudio examinó 24 cadáveres adultos para determinar la ubicación de la RCDNI en el músculo deltoides. Se trazó una línea de referencia longitudinal (línea L) entre el acromion y el epicóndilo lateral del húmero, y una línea de referencia transversal semicircular (línea H) desde el punto más bajo de la incisura yugular, pasando por el acromion, hasta el extremo medial de la espina

de la escápula. Se utilizó la tinción de Sihler para visualizar las regiones intramusculares con alta densidad de nervios, y se aplicó sulfato de bario para marcar la región intramuscular con alta densidad de nervios. Se emplearon tomografías computarizadas (TC) helicoidales y el sistema Syngo para registrar el punto de proyección de la región intramuscular con alta densidad de nervios en la superficie corporal, denominado punto P. La intersección de la línea vertical que pasa por el punto P con la línea H y la línea horizontal con la línea L se denominaron PH y PL, respectivamente. Se midieron y analizaron los porcentajes de posición de PH y PL a lo largo de las líneas H y L, así como la profundidad de la región intramuscular con alta densidad de nervios. Las porciones anterior, media y posterior del músculo deltoides contenían una zona intramuscular con alta densidad de nervios bien definida. Los puntos PH del CINDR se ubicaron al 45,52 %, 54,76 % y 76,19 % a lo largo de la línea H, mientras que los puntos PL se ubicaron al 18,99 %, 23,65 % y 22,16 % a lo largo de la línea L. Las profundidades del CINDR fueron de 1,08 cm, 1,99 cm y 1,44 cm, respectivamente. Todos los porcentajes representan valores medios. Las ubicaciones del CINDR identificadas deben evitarse durante las inyecciones intramusculares de fármacos de rutina y deben servir como objetivos efectivos para los procedimientos de adelgazamiento de hombros con toxina botulínica y el tratamiento de espasmos musculares.

PALABRAS CLAVE: Músculo deltoides; Inyecciones; Nervios intramusculares; Toxina botulínica; Tomografía; Tomografía computarizada espiral.

REFERENCES

- Amirali, A.; Mu, L. C.; Gracies, J. M. & Simpson, D. M. Anatomical localization of motor endplate bands in the human biceps brachii. *J. Clin. Neuromuscul. Dis.*, 9(2):306-12, 2007.
- Behringer, M.; Franz, A.; McCourt, M. & Mester, J. Motor point map of upper body muscles. *Eur. J. Appl. Physiol.*, 114(8):1605-17, 2014.
- Borodic, G. E.; Ferrante, R.; Pearce, L. B. & Smith, K. Histologic assessment of dose-related diffusion and muscle fiber response after therapeutic botulinum A toxin injections. *Mov. Disord.*, 9(1):31-9, 1994.
- Cohen, J. M. & Gray, A. T. Functional deficits after intraneural injection during interscalene block. Reg. Anesth. Pain Med., 35(4):397-9, 2010.
- Charmode, S.; Sharma, S.; Kushwaha, S. S.; Mehra, S.; Sangma, S. S. & Mishra, V. Deltoid intramuscular injections: a systematic review of underlying neurovascular structures to the muscle and proposing a relatively safer site. *Cureus*, 14(4):e24172, 2022.
- Desai, K.; Warade, A. C.; Jha, A. K. & Pattankar, S. Injection-related iatrogenic peripheral nerve injuries: surgical experience of 354 operated cases. *Neurol. India*, 67(Supplement):S82-S91, 2019.
- Gentili, F.; Hudson, A. R.; Kline, D. & Hunter, D. Early changes following injection injury of peripheral nerves. Can. J. Surg., 23(2):177-82, 1980.
- He, X.; Li, Y.; Wang, J.; Hu, S.; Wang, M. & Yang, S. Localization of the centre of the highest region of the triceps brachii muscle spindle abundance and its significance in muscle spasticity block. *Int. J. Morphol.*, 40(4):1100-7, 2022.
- He, X. J.; Wen, S. F.; Liu, X.; Li, Y. T. & Yang, S. B. Optimal target localization for botulinum toxin A in treating splenius muscles dystonia based on the distribution of intramuscular nerves and spindles. *Anat. Sci. Int.*, 2025. Doi: https://doi.org/10.1007/s12565-025-00831-8
- Hu, X. N.; Wang, M.; He, X. J.; Chen, P.; Jia, F. F.; Wang, D. L. & Yang, S. B. Division of neuromuscular compartments and localization of the center of the intramuscular nerve-dense region in pelvic wall muscles based on Sihler's staining. *Anat. Sci. Int.*, 99(1):127-37, 2024.
- Kakati, A.; Bhat, D.; Devi, B. & Shukla, D. Injection nerve palsy. *J. Neurosci. Rural Pract.*, 4(1):13-8, 2013.
- Kim, Y. G.; Chung, Y. H.; Ahn, H. J.; Jeon, A.; Kim, Y. S.; Hwang, K. & Han, S. H. Thickness of the deltoid muscle and location of the anterior branch of the axillary nerve and the posterior circumflex humeral artery for deltoid injections. *Biomed. Res. Int.*, 2022:1784572, 2022.

- Koh, Y. G.; Shin, S. H.; Kim, K. R.; Yeoum, S. H.; Choi, W. W. & Park, K. Y. A double-blinded, randomized, dose-comparison pilot study to comparatively evaluate efficacy and safety of two doses of botulinum toxin type A injection for deltoid muscle hypertrophy. *Ann. Dermatol.*, 35(5):355-9, 2023.
- Larionov, A.; Yotovski, P.; Link, K. & Filgueira, L. Innervation of the clavicular part of the deltoid muscle by the lateral pectoral nerve. *Clin. Anat.*, 33(8):1152-8, 2020.
- Lewis, J. Rotator cuff related shoulder pain: assessment, management and uncertainties. Man. Ther., 23:57-68, 2016.
- Pandian, J. D.; Bose, S.; Daniel, V.; Singh, Y. & Abraham, A. P. Nerve injuries following intramuscular injections: a clinical and neurophysiological study from Northwest India. J. Peripher. Nerv. Syst., 11(2):165-71, 2006.
- Parratte, B.; Tatu, L.; Vuillier, F.; Diop, M. & Monnier, G. Intramuscular distribution of nerves in the human triceps surae muscle: anatomical bases for treatment of spastic drop foot with botulinum toxin. *Surg. Radiol. Anat.*, 24(2):91-6, 2002.
- Picelli, A.; Vallies, G.; Chemello, E.; Castellazzi, P.; Brugnera, A.; Gandolfi, M.; Baricich, A.; Cisari, C.; Santamato, A.; Saltuari, L.; et al. Is spasticity always the same? An observational study comparing the features of spastic equinus foot in patients with chronic stroke and multiple sclerosis. J. Neurol. Sci., 380:132-6, 2017.
- Pinho, S.; Camões-Barbosa, A.; Hatia, M.; Moeda, F.; Melo, X. & Tocha, J. Shoulder spasticity treatment with botulinum toxin: a nationwide crosssectional survey of clinical practices. *Cureus*, 15(11):e48493, 2023.
- Shin, S. H.; Park, S. J.; Yeoum, S. H.; Youn, C. S. & Park, K. Y. Efficacy and safety of botulinum toxin injection in reducing deltoid muscle hypertrophy. *Dermatol. Ther.*, 34(6):e15168, 2021.
- Stecco, C.; Gagliano, G.; Lancerotto, L.; Tiengo, C.; Macchi, V.; Porzionato, A.; De Caro, R. & Aldegheri, R. Surgical anatomy of the axillary nerve and its implication in the transdeltoid approaches to the shoulder. *J. Shoulder Elbow Surg.*, 19(8):1166-74, 2010.
- Stokey, P. J.; Kaur, S.; Lee, A.; Behrens, K. & Ebraheim, N. Anatomy and deficiency of the deltoid muscle: a review of literature. *Orthop. Rev. (Pavia)*, 16:115352, 2024.
- Van Gelein Vitringa, V. M.; Jaspers, R.; Mullender, M.; Ouwerkerk, W. J. & Van Der Sluijs, J. A. Early effects of muscle atrophy on shoulder joint development in infants with unilateral birth brachial plexus injury. *Dev. Med. Child Neurol.*, 53(2):173-8, 2011.
- Van Ouwenaller, C.; Laplace, P. M. & Chantraine, A. Painful shoulder in hemiplegia. Arch. Phys. Med. Rehabil., 67(1):23-6, 1986.
- Wang, D. L.; Chen, P.; Jia, F. F.; Wang, M.; Wu, J. X. & Yang, S. B. Division of neuromuscular compartments and localization of the center of the highest region of muscle spindle abundance in deep cervical muscles based on Sihler's staining. Front. Neuroanat., 18:1340468, 2024.
- Wang, J.; Li, Y. R.; Wang, M. & Yang, S. B. Localization of the center of the intramuscular nerve-dense region of the suboccipital muscles: an anatomical study. Front. Neurol., 13:863446, 2022.
- Yi, K. H.; Choi, Y. J.; Lee, J. H.; Hu, H.; Gil, Y. C.; Hu, K. S. & Kim, H. J. Anatomical considerations for the injection of botulinum neurotoxin in shoulder and arm contouring. *Aesthet. Surg. J.*, 44(3):319-26, 2024.
- Yi, K. H.; Lee, J. H.; Hu, H.; Park, H. J.; Lee, H. J.; Choi, Y. J. & Kim, H. J. Botulinum neurotoxin injection in the deltoid muscle: application to cosmetic shoulder contouring. Surg. Radiol. Anat., 45(7):875-80, 2023.

Corresponding author:
Shengbo Yang
Department of Anatomy
Zunyi Medical University
6 University West Road
Xinpu New Developing Areas
Zunyi City
Guizhou Province 563099
CHINA

E-mail: yangshengbo8205486@163.com